**ELUSIVE FORMATION OF IMPACT BASINS ON THE YOUNG MOON.** Katarina Miljković[1,2], Mark A. Wieczorek[3], Matthieu Laneuville[4], Phil A. Bland[1], and Maria T. Zuber[2]. [1]Department. of Applied Geology, Curtin University, Perth, Australia (katarina.miljkovic@curtin.edu.au); [2]Department of Earth, Atmospheric and Planetary Sciences, Massachusetts Institute of Technology, Cambridge, MA 02139, USA; [3]Laboratoire Lagrange, Observatoire de la Côte d'Azur, Nice, France; [4]Earth-Life Science Institute (ELSI), Tokyo Institute of Technology, Japan.

**Introduction:** The Moon-forming impact event [e.g., 1], estimated to have occured ~4.54-4.42 Gyr ago [e.g., 2] left the Moon with a thick lunar magma ocean (LMO) [3]. The LMO crystallization timeframe could have been as short as 50 Myrs [e.g., 2,4] or prolonged due to tidal effects for 200 Myrs or more [5-6]. During the early LMO solidification period, the flotation crust formed, up to 50 km in thickness [e.g., 2,4-5].

The last cumulates to crystalize were ilmenite and KREEP-rich rocks [e.g., 7] that localized beneath the thinnest crust on the lunar nearside hemisphere, within the Procellarum KREEP Terrane (PKT) [e.g., 8]. The radiogenic heating from the KREEP-rich layer would have increased ambient temperatures such that the entire layer was likely to have been completely molten during the first 500 Myr after lunar formation [8].

Here we show that, depending on the thickness of the lunar magma ocean at the time of impact, basins form as completely or partially relaxed in morphological structure. The only exception was the South Pole-Aitken (SP-A) basin, that retained clear evidence of an impact likely because of its size.

**Observations:** The GRAIL-gravity survey produced an updated lunar impact basin catalogue [9]. A typical impact basin constitutes a Bouguer anomaly associated with the uplift of the underlying mantle that is denser than the crust. Pre-Nectarian impact basins listed in [9] as accepted impact basins show smaller Bouguer anomalies compared to younger impact basins of similar size, which indicates that the oldest basins have the most relaxed morphology.

The SP-A basin is the oldest and largest impact basin on the Moon. It is elliptical in shape, with best-fit axes measuring 720 by 920 km and outer topography axes 1028 by 1200 km [10]. Unlike other impact basins, the SP-A basin is nearly isostatically compensated; its inner depression is ~13 km deep [10] and the radius of the zone of crustal thinning extends up to about 700 km followed by a nearly indistinguishable thickening up to 1200 km [11] (Fig. 1).

**Method:** We used the iSALE-2D shock physics hydrocode [12-13] to study the relaxation properties of impact basins depending on target properties, as it occurred during a basin formation event. Impact simulations were made into a flat (for smaller impacts) or curved lunar target (for larger impacts, including the SP-A basin). Target was divided into three stratigraphic layers: 1) 30-km-thick cold conductive crust, 2) 10, 25 or 50 km thick inviscid or viscoelastic (with low viscosity) interface layer that represented partially or completely molten material (viscosity up to ~100 Pas, typical for molten ultramafic basaltic rock [e.g., 14]), and 3) solid upper mantle.

In this work, we considered two radial temperature profiles. The "hot" profile is the same as hot initial mantle used in thermal evolution models [15] and the "cold" profile had a 50 K/km initial gradient followed by a cooler adiabat starting from below the crust. The impactor ranged from 30 to 200 km in diameter. The impact velocity typical for the Moon was either 10 km/s or 17 km/s [e.g., 16 and refs therein].

**Preliminary results** show that completely relaxed impact basins form in targets with at least 25 km-thick interface layer, regardless of the target temperature, for all typical lunar basin sizes, except SP-A. The relaxation is reached within a few hours after impact by a thick crustal inflow as the final modification during basin formation. However, partly relaxed impact basins form when the interface layer is approximately 10-25 km thick, for the entire range of lunar basin sizes. If the interface layer is <10 km thick, final basin morphology is the same as if there were no melt layer between the crust and the mantle.

**The South Pole-Aitken basin** was also simulated to have formed on the young Moon while the LMO was still solidifying. We used a 30-km-thick pre-impact crust, a 25-km thick interface layer overlying the solid mantle, and the impactor was 200 km in diameter, moving at 10 km/s, as in [17]. The results for the SP-A formation are shown in Figs 1-3.

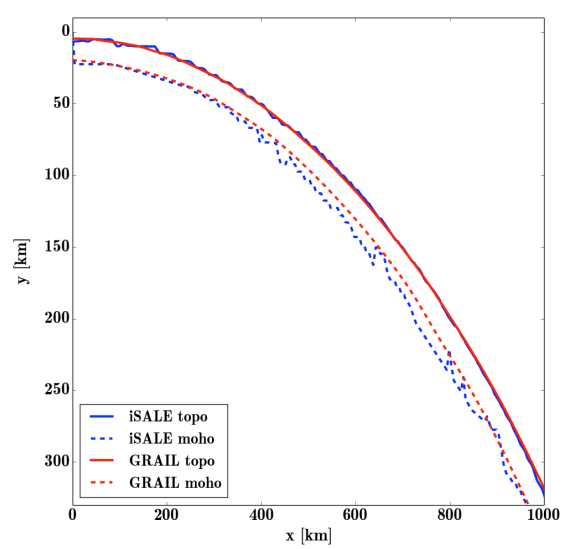


**Figure 1.** Comparison of the topographic and crust-mantle interface profiles between remote sensing data

obtained by LOLA and GRAIL, shown in red [11] and the results from a numerical simulation 3 hours after impact (shown in blue).

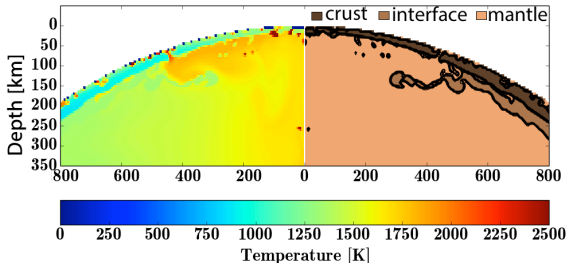


**Figure 2.** The SP-A basin showed in temperature contour plot (left) and material location (right).

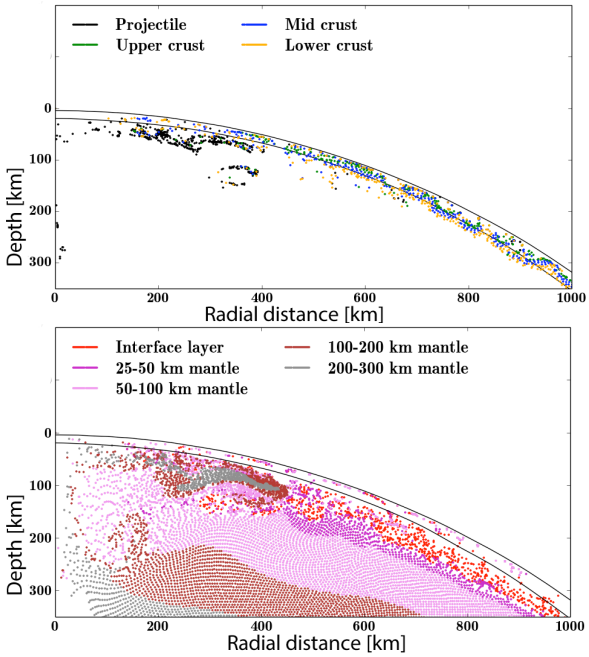


**Figure 3.** Coarse distribution of tracer particles post impact show crust (top) and mantle (bottom) stratigraphy in the SP-A basin, including projectile contribution (top). Black lines are LOLA and GRAIL-derived topographic and crust-mantle interface profiles [11].

Preliminary results suggest that regardless of the target and impactor properties, the final basin morphology is different, compared to the majority of impact basins as observed by GRAIL, as long as the interface melt layer was present at the time of their formation.

Most lunar impact basins show distinctive positive Bouguer anomalies associated with the uplift of the underlying mantle. The ratio of the thickness of the crustal cap in the center of a basin and the ambient thickness is 0.8-0.9 for the smallest impact basins, which decreases steadily down to 0.2 for the largest (Nectarian and Imbrian) basins [9,16]. Basins that formed on the young Moon show a less pronounced mantle uplift preserved in the crust and a prominent crustal inflow that covered the crater site. The above-mentioned ratio is close to 1 for completely relaxed and around 0.5 for partly relaxed basins, for the entire range of basin sizes. This effectively created a lower density contrast to be observed in gravitational surveys. In the case of the SP-A basin, its crustal profile as observed today could have entirely formed during the basin formation process.

Large impacts on the young Moon show that impact-generated melt and the projectile emplaced underneath the crustal cap (Figs. 2-3), instead of becoming majorly exposed on the surface as shown in [17] for the SP-A basin. In the case of the SP-A basin, a contribution from the deeper mantle could also feed into the interface layer (Fig 3).

The ejecta is composed of overturned, heavily mixed and fractured crust (Fig. 3 top). In larger impacts, a small contribution from the interface layer and possibly upper mantle is possible on the surface (Fig. 3 bottom). For the SP-A basin, it could account for the mafic anomany observed in the inner depression [18]. Simulations also show that the SP-A ejecta is largely contained within the outer basin radius.

**Conclusion:** Lack of an early lunar cratering record does not indicate lack of impact bombardment on the Pre-Nectarian Moon and Hadean Earth. In fact, this work shows that for target properties expected for the earliest Moon, typical basin formation (except SP-A) was unlikely to form a morphologic structure retainable to present day.

**References:** [1] Canup R.M. et al. (2001) *Nature 412,* 708–712. [2] Elkins-Tanton L.T. et al. (2011) *Earth Planet. Sci. Lett. 304,* 326–336. [3] Tonks W.B. and Melosh H.J. (1993) *J. Geophys. Res. 98,* E3, 5319–5333. [4] Shearer C.K. et al. (2006) *Rev. Mineral. Geochem. 60,* 365–518. [5] Meyer, J. et al. (2010) *Icarus 2008,* 1–10. [6] Ćuk et al. (2016) *Nature 539*, 402–406. [7] Hess P.C. and Parmetier E.M. (1995) *Earth Planet. Sci. Lett. 134,* 501–514. [8] Wieczorek M.A. and Philips R.J. (2000) *J. Geophys. Res. 105*, 20,417–20,430. [9] Neumann G.A. et al. (2015) *Sci. Adv. 1*, 9, e1500852. [10] Gerrick-Bethell I. and Zuber M.T. (2009) *Icarus 204*, 399–408. [11] Wieczorek M.A. et al. (2013) *Science 339,* 671–675. [12] Amsden A.A. et al. (1980) *LANL report* LA-8095, 105. [13] Collins G.S. et al. (2004) *Meteorit. Planet. Sci. 39,* 217–231. [14] Reese C.C. and Solomatov V.S. (2006) *Icarus 184*, 102–120. [15] Laneuville M. et al. (2013) *J. Geophys. Res 118,* 1435–1452. [16] Miljković K. et al. (2015) *J. Geophys. Res. 121*, 1695–1712. [17] Potter R.W.K. et al. (2012) *Icarus 220*, 730–743. [18] Jolliff B.J. et al. (2000) *J. Geophys. 105*(E2), 4197–4216.

**Acknowledgements:** KM thanks TIGeR for funding support. We gratefully acknowledge the developers of iSALE-2D (www.isale-code.de/projects/iSALE).